Journal of Hazardous Materials 172 (2009) 54–60

Contents lists available at ScienceDirect

Journal of Hazardous Materials

journal homepage: www.elsevier.com/locate/jhazmat

Axial temperature distribution in vertical jet fires

Mercedes Gómez-Mares*, Miguel Muñoz, Joaquim Casal

Centre for Technological Risk Studies (CERTEC), Department of Chemical Engineering, Universitat Politècnica de Catalunya, Diagonal 647, 08028 Barcelona, Spain

ARTICLE INFO

Article history:
Received 9 December 2008
Received in revised form 23 June 2009
Accepted 23 June 2009
Available online 3 July 2009

Keywords:
Fire
Jet fire
Flame temperature
Temperature distribution

ABSTRACT

The behaviour of vertical commercial propane jet fires (flame lengths of up to 8 m) was studied experimentally. The temperatures along the jet fire centreline were measured using a set of thermocouples and the flame contour was determined from infra-red (IR) images. The results show that temperature increases from the bottom of the flame, reaches a maximum value and decreases again at the top zone. A second-degree polynomial expression describes fairly well the variation of temperature as a function of the position on the flame centreline. The temperature along the centreline was found to increase for Q values lower than 7 MW and to decrease at higher values.

© 2009 Elsevier B.V. All rights reserved.

1. Introduction

Fires are the most frequent major accidents that occur in process and storage plants and during the transportation of hazardous materials. The ratio between occurrence of fires, explosions and toxic clouds in these accident scenarios is approximately 10:6:1 [1]. Although the adverse effects of fires are usually confined to a smaller area than in the case of explosions and toxic releases, the affected area often contains other equipment that can be seriously damaged by the thermal flux [2–4] which creates a domino effect.

A jet fire is a specific type of fire that occurs when a high-velocity leak of gas or two-phase flow is ignited. Jet fires can occur when a pipe is broken, when a hole forms in a tank, when gas leaks from a flange, or when a safety valve is opened. Although most jet fires are caused by LPG leakage, they have also occurred with different hydrocarbons depending on the process conditions.

Jet fires are generally smaller than other types of fires in accident scenarios, but they often produce very high heat fluxes, particularly if the flames reach surrounding equipment. Consequently, jet fires can cause catastrophic failures in a very short period of time. In some cases, serious explosions have occurred only 70 s after a jet fire reached a tank. A recent study by Gómez-Mares et al. [5] reports that approximately 50% of the recorded cases of jet fires are followed by additional severe events. This is an extremely important factor because it means that the scale of an accident may increase considerably when a jet fire occurs.

This type of fire has not been researched in detail, especially in regards to the temperature fields, and most predictions of the effects of jet fires have been derived from flares or horizontal jet flames [3,4]. Various authors have analysed the shapes and sizes of jet fires [6–8], and some research into their thermal characteristics has been performed (some examples are [6–11]). However, some of these studies have been performed with subsonic jets, whereas most accidental jet fires are sonic. There is particularly scarce information on specific aspects such as temperature distribution [6–11]. This is probably due to the difficulties associated to such type of measurements. Furthermore, the experimental data available on this subject are mainly taken from small-scale jet flames analysed in laboratory conditions, and the extrapolation to large-scale real jet fires probably implies a significant degree of error.

In this paper, experimental data for large vertical sonic jet fires (flame lengths of up to 9 m) are presented and an expression for predicting the axial fire temperature is formulated.

The knowledge of the temperature variation can be useful for a better prediction of the thermal radiation intensity from a jet fire. Usually this is done by applying the solid flame model and assuming a constant value of the emissive power (which is a function of temperature) over the whole jet fire. However, the emissive power is not constant and varies with the flame length. Therefore, a multiple zone (for example, a three-zone) model would improve the thermal radiation prediction, especially for short distances (where significant fire effects exist). Furthermore, the availability of experimental data from large-scale jet fires is essential

* Corresponding author. Tel.: +34 934016675; fax: +34 934017150.
E-mail address: m.gomez.mares@upc.edu (M. Gómez-Mares).

0304-3894/$ – see front matter © 2009 Elsevier B.V. All rights reserved.
doi:10.1016/j.jhazmat.2009.06.136

Nomenclature

a	coefficient in Eq. (2)
A	coefficient in Eq. (3)
b	coefficient in Eq. (2)
B	coefficient in Eq. (3)
c	coefficient in Eq. (2)
C	coefficient in Eq. (3)
d	jet outlet diameter (m)
L	visible flame length (lift-off length not included) (m)
m	fuel mass flow rate (kg s^{-1})
p	percentage of axial position, z/L
P_0	atmospheric pressure (bar)
P_{in}	pressure inside the tank or pipeline (bar)
Q	nominal heat release rate (MW)
R^2	or SQR, coefficient of determination
t	time (s)
T	flame temperature (K)
z	distance from the thermocouple location to the bottom of the flame (m)

for the validation of computational fluid dynamics (CFD) modelling.

2. Previous work

Little research has been carried out into the temperature distribution in jet fire flames, and available data do not identify clear patterns. Some measurements are reported but no equations are established for predicting the temperature, with the exception of the McCaffrey equation [7]. This scarcity of data can be attributed to the fact that it is difficult to measure the temperatures in large-scale jet flames. Jet fires are highly turbulent, so the shape and structure of the flame can vary very quickly and the inertia and response velocity of the thermocouples can mask the real temperature variation. In addition, prevailing weather conditions affect the composition of the oxygen/fuel mixture and the position and shape of the flame. Consequently, the data obtained by the thermocouples are often scattered [6,7,10].

The literature contains generally average flame temperatures and some average maximum temperatures, which were generally measured at the jet centreline [6–8,10,11]. However, the temperature of a jet fire changes considerably according to the position at which measurements are taken.

Most of these data were recorded for small size jet fires or subsonic flames [7,8,10,11]. However, the exit velocity is sonic in most real jet fires; for most gases, sonic velocity is reached at the vessel/pipe outlet when $P_{in}/P_0 > 1.9$, and this condition is met by many storage tanks and pipes.

Brzustowski et al. [10] studied laboratory-scale propane flares affected by a crosswind. They measured the temperature of the flame centreline. The presentation of the results was complex; the authors plotted transverse and horizontal temperature profiles. The maximum temperature was approximately 1500 K.

Becker and Yamazaki [11] measured the maximum average flame centreline temperature of small-scale ($L < 2.5$ m) propane jet flames (approximately 1700 K, located in an axial position at 60% of the flame length). Several plots were shown: temperature profiles at various relative axial positions, and mean temperatures as a function of axial and radial positions.

Sonju and Hustad [6] studied the average temperature of methane and propane jet flames, but they did not indicate the exact measurement position. For small-scale methane flames ($L < 1$ m) they provided a temperature contour plot that showed a mean centreline temperature of 1820 K, and for small-scale propane flames they gave a maximum temperature of 1570 K. For large-scale flames they measured the maximum average centreline temperatures for propane (1070–1470 K) and methane (1270–1420 K).

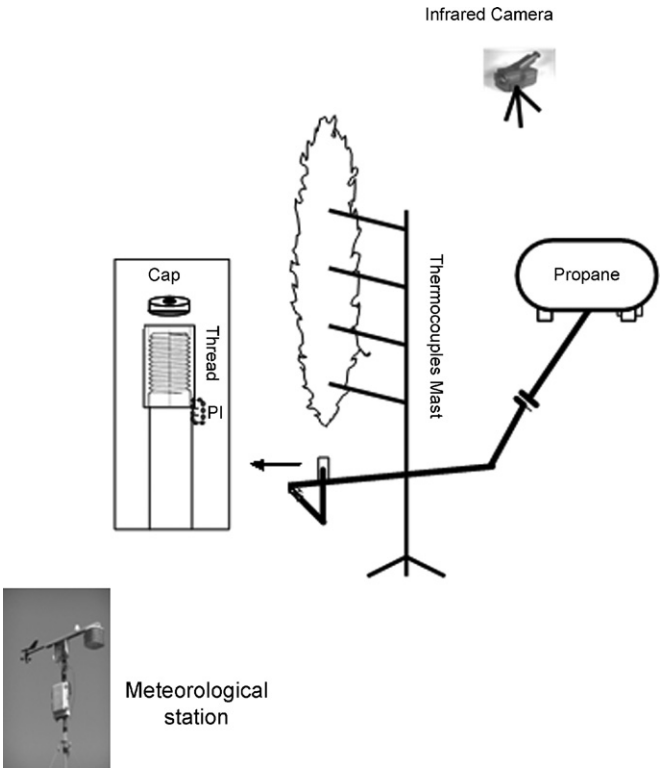

Fig. 1. Experimental set-up.

Pfenning [9] published a detailed study of large-scale natural gas flames (flame length of 20 m). He found that the maximum temperature for this type of jet flame was approximately 1250 K, measured at the centre of the flame. A couple of years later, Gore et al. [12] analysed these data providing temperature profiles for some vertical natural gas diffusion flames.

McCaffrey [7] conducted experiments with methane flames (flame length up to 7 m). He found that the average maximum centreline temperature for this type of flame was approximately 1220 K and that the value was recorded between 20% and 60% of the flame length (measured from the bottom). He also obtained a temperature correlation as a function of the heat release, over a given range of values of mass flow rate, observing an increasing trend of T as a function of Q.

More recently, Santos and Costa [8] studied the maximum average temperature of small propane and ethylene vertical jet flames (flame length of 1.6 m). The maximum average temperatures ranged between 1300 and 1500 K for the propane flames and between 1500 and 1700 K for ethylene.

2.1. Experimental set-up

The experimental facility used in this study was built at the Can Padró Safety Training Centre located near Barcelona, Spain. A schematic representation of the field test apparatus is shown in Fig. 1. The facility consisted of a set of pipes which produced vertical jet fires with sonic and subsonic exit velocities (Fig. 2).

The gas pipe outlet had a removable cap, which was used to adjust the outlet diameter. Five diameters were used: 12.75, 15, 20, 25.5, and 30 mm. The burner exit was directed vertically upward at a height of 0.5 m above the ground. Pressure measurements

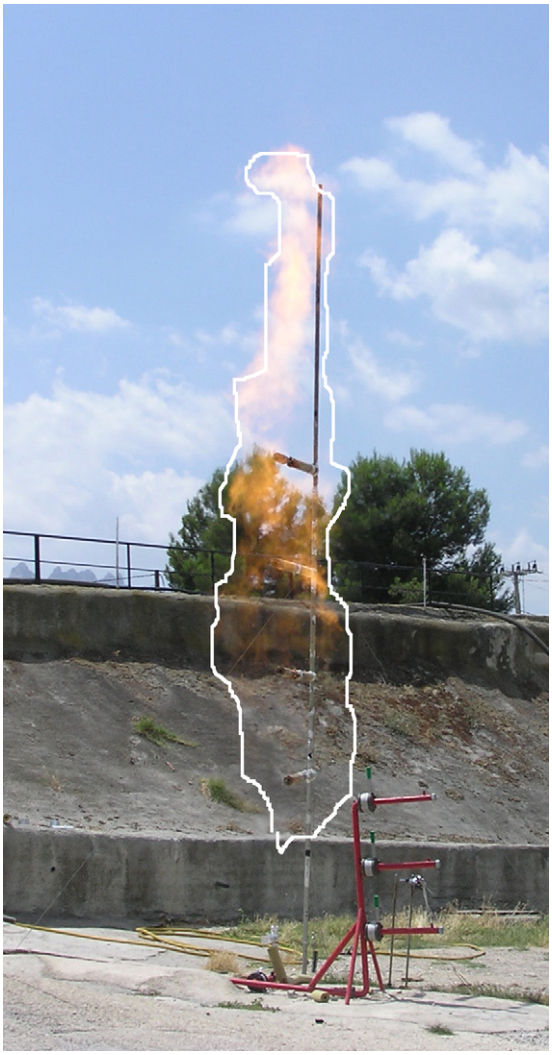

Fig. 2. A vertical jet of propane (sonic flow). The contour of the flame has been indicated.

were taken at the gas outlet to calculate the mass flow rate (m). The stagnation pressure varied in the different tests, and therefore the density of the released gas changed correspondingly. Thus, although the linear velocity was constant and equal to the sonic velocity, the mass flow rate changed. The fuel (commercial propane) was contained in a pressurised tank (4 m^3). The liquid propane was vaporized as it flowed through the pipe.

The propane pressure (P_{in}) was measured at a point located 5 cm upstream of the release point using an electronic pressure transmitter. The value recorded was taken as the upstream stagnation pressure of the flow.

In this study, an AGEMA 570 infrared thermographic camera located orthogonally to the flame was used to determine the main geometric parameters of the jet (due to the fact that the flame can be transparent sometimes, it can be impossible or very difficult to analyse it with a common video camera). This type of camera has a focal plane array (FPA) detector of 320 × 240 pixels, which is sensitive to radiation at a certain wavelength. The spectral range of the model used in this study was 7.5–13 μm, and the field of vision was 24° × 18°. Although the IR measurements can be used to compute the flame temperatures, these data will not be analysed in this paper; however, these images were used to determine the flame length.

Type B (Pt 30% Rh/Pt 6% Rh) and S (Pt 13% Rh/Pt) uncoated thermocouples (0.35 mm diameter) were used to measure the axial temperature distribution of the flames because they are able to detect higher temperatures than thermocouples with a different metal couple. The error of the type B thermocouples was 0.5 over 1070 K and for the type S thermocouple, 1.5 K, according to the data provided by the supplier (the equipment calibration was carried out by the company which sold the instruments). The four thermocouples were arranged on a mast at 1.8, 2.6, 3.6 and 4.5 m from the floor, as shown in Fig. 1. This distribution was chosen in an attempt to cover all the flame regions, taking into account the lift-off of the flame. An additional thermocouple was also placed at the jet outlet. The appropriate thermodynamic relationships were applied to calculate the fluid velocity at the outlet. No correction for the radiation error was applied; however, taking into account the location of the thermocouples (inside the jet fire) the error should be negligible [13,14].

A GroWeather meteorological station console was used to provide continuous measurements of the ambient temperature, the relative humidity and the wind direction and velocity. These variables may directly or indirectly affect both the jet flame and the measurement instruments. A FieldPoint module was used for data acquisition. It consisted of a FP-1001 communication module (RS-485, 115 kbs^{-1}), three FP-TB-1 connection terminals and three input/output (I/O) modules. An RS-485 communication port was used to connect the I/O modules to the FP-1001 module, which was connected to the computer and the power supply.

The FP-TB-1 terminal connection bases were used to support the I/O modules. They guaranteed a constant power supply and served as an internal communication system between the I/O and FP-1001 modules.

Two of the I/O modules were FP-TC-120 modules. The thermocouples were connected to one of these modules and the measurements were stored by the computer. The other I/O module was of type FP-AI-110 and was used to collect the information generated by the pressure transmitter.

Two laptops were used to collect the data from the different sensors and to control the operation of the measurement devices. They were connected to the IR camera, the meteorological station and the FieldPoint module, and were linked via a network to synchronize the data acquisition.

The FireAll software [15] created at CERTEC to manage the operation of the devices used in experiments was installed on the computers. It was used to synchronize the point at which the computers start to record measurements, and made the data easier to analyse by generating separate files for each experiment and synchronizing the measurements.

2.2. Test conditions

A total of twenty experiments were carried out, of which only the momentum dominated sonic gas flames were selected and analysed. The procedure consisted of opening a valve which allowed the propane flow through the pipeline. The propane, contained in the pressurized tank, was vaporized as it flowed through the pipe up to the outlet. Downstream the gas outlet, an ignition source ignited the gas jet. The duration of each experiment was variable, depending on the time required by the flame to reach the steady state, but the duration of each trial was between 1 and 5 min, covering a wide range of mass flow rates. The instruments provided four measurements per second. Ambient temperature ranged between 300 and 305 K, and relative humidity between 45% and 53%. The experiments were carried out in calm (no wind) conditions. The nozzle exit Reynolds number ranged between 8×10^5 and 3×10^6, which means that all the flames were on the turbulent regime. The Froude number was always greater than 2.4×10^5. Information regarding

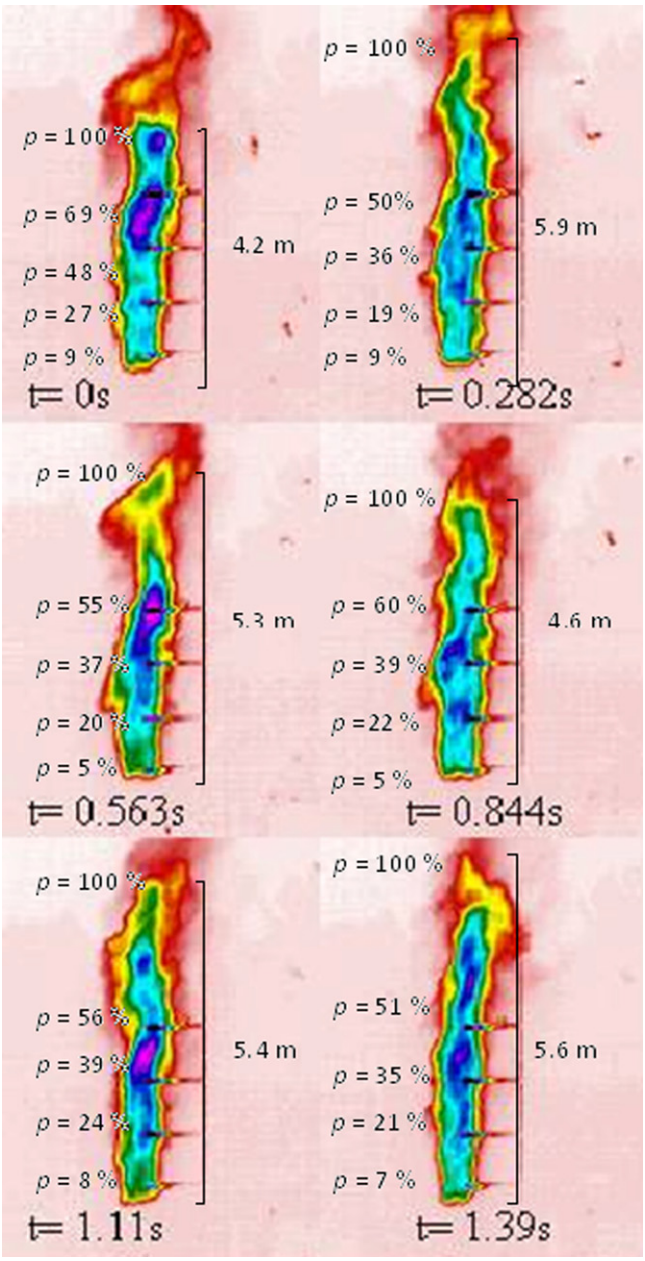

Fig. 3. A sequence of jet fire IR images.

geometric parameters of the flame (i.e. flame length and lift-off) can be found in another paper [16]. As a reference, the length for flames from 2.7 to 7.4 MW ranged between 3 and 5 m; from 7.8 to 13.8 MW, 3 m $\leq L \leq$ 7 m and from 14.7 to 19.7 MW, 4 m $\leq L \leq$ 8 m. The lift-off height for all the flames analysed in this paper ranged between 0.65 and 1 m.

3. Flame temperature as a function of axial position

A set of vertical propane jet flame experiments was analysed to determine the temperature variation as a function of the axial position. A wide range of jet flame sizes (not including the lift-off height) were considered (from 3 to 8 m). The propane mass flow rate ranged between 0.06 and 0.43 kg/s or, expressed as a function of the theoretical heat released rate Q, from 3 to 19.7 MW. The flame length was measured by analysing the IR images, which showed clearly (see Fig. 3) the boundaries of the flame. The IR video was analysed frame by frame (4 frames per second), and for each frame the distance in pixels between the bottom and the tip of the flame was determined and after converted to meters, using reference distances such as the distance between thermocouples. The flame boundaries (bottom and tip) were determined assuming that the flame has temperatures higher than 800 K (threshold). Note that the bottom of the flame is just above the end of the lift-off. Regions with lower temperature were considered as hot gases. More than 900 images were analysed. IR images were used instead of the images filmed by the video camera because sometimes the flame is outside the visible spectrum range, as can be observed in Fig. 2. The jet flame length was proportional to the mass flow rate, so higher mass flow rates produced longer flames.

The temperature profile of sonic vertical jet flames was obtained by analysing the temperatures measured by the thermocouples. Although other measurement techniques exist (as, for example, optical measurement [17] or IR images [15]), in this study only the thermocouples measurements were considered. Future work will be carried out to analyse the IR images considering them as a source for getting temperature and radiation zones.

The first step consisted in determining the exact position of each thermocouple in the flame at each instant. This is a difficult task due to the turbulence and the continuous variation in flame size. The IR video was broken down again frame by frame (4 fps) and the position of each thermocouple relative to the flame was determined and associated to the corresponding temperature at that instant. As the position of the flame (bottom of the flame) changed, it was necessary to determine the exact relative position of each thermocouple for each image. The axial position of the thermocouples was considered as a percentage and was obtained by dividing z, the distance between the location of the thermocouple and the bottom of the flame, by L, the radiant flame length (not including the lift-off height). The axial position $p = 0\%$ was taken to be the base of the flame, and the axial position $p = 100\%$ the flame tip. When plotted against the temperature, this parameter, p, gives a good picture of how the temperature varies with flame axial position, much clearly than if z/d was used. To completely define the flame position with respect to the release point, the lift-off distance is required; expressions to estimate it can be found in [16].

The fuel mass flow rate m as well as the nominal heat release rate Q were also calculated for each instant. Only images of jet fires with a sonic outlet velocity were considered.

The data were analysed for each Q and it was generally found that the flame can be divided into three regions according to temperature behaviour.

In Region I ($p < 40\%$) the temperature increased with the axial position reaching values of approximately 1800 K. In Region II ($40 \leq p \leq 70\%$), the temperature profile showed a smooth variation: the average value of T remained close to 1800 K and the maximum temperatures were found (up to 1900 K in some cases). Finally, in Region III ($p > 70\%$) the temperature began to decrease, although higher temperatures were recorded at the tip of the flame than at its bottom. Of course, the temperatures found are always lower than the adiabatic temperature of a propane flame (2470 K) [18].

Fig. 4 shows the plot of a typical case in which this behaviour is observed, where $d = 12.75$ mm and the flame length is 4.2 m. The temperatures at the base of the flame are approximately 1300 K, reaching a maximum of 1900 K at approximately $p = 60\%$ and then decreasing to 1700 K near to the flame tip. The scattering of the experimental data is relatively large due to the turbulence and the aforementioned measurement difficulties. However, the general pattern of the temperature variation is clear.

This behaviour can be accounted for by the air/fuel mixture and the heat balance. In Region I, the mixing of air and fuel is starting and therefore the oxygen/fuel mixture is still poor in oxygen; thus, the burning velocity is relatively low over this region and

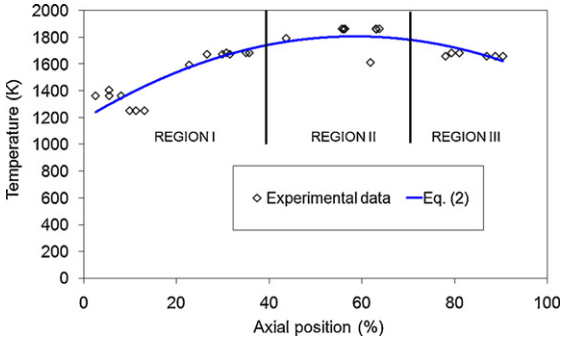

Fig. 4. Temperature variation as a function of the axial position in the flame (Q = 6.4 MW, d = 12.75 mm).

the temperatures reached are lower than those found in Region II, where there is a better combustion. In addition, the gas entering the region is cold so the temperatures are relatively low. In Region II the conditions are much more favourable: the gas entering the region is hot (except for the air entrained through the flame contour) and the ratio oxygen/fuel is close to the stoichiometric value (a high dilution of propane is required to reach a flammable mixture: LFL = 2.1%, UFL = 9.5% vol), so higher temperatures are reached. Finally, in Region III a significant amount of the fuel has already been consumed, so the amount of heat released is lower and fresh air continues to enter the jet, which causes the temperature to decrease again.

We tried to define an empirical expression for predicting this centreline temperature profile. A range of expressions were tested, including polynomial equations of several degrees, lineal, exponential and logarithmic expressions. The best agreement was found with a second-degree polynomial, which had the highest R^2 and gives the temperature at each point as a function of the axial position on the flame centreline, as shown below:

$$T = a + bp - cp^2 \quad (1)$$

The agreement between the experimental data and this expression can be seen in Fig. 4. The plotted line represents the best polynomial regression found. As can be observed, although there is a certain degree of scattering (R^2 = 0.8), the experimental data correlate well with the following expression:

$$T = 1190 + 21.2p - 0.18p^2 \quad (2)$$

where T is the temperature in K and p is the axial position expressed as a percentage.

Fig. 5 shows polynomial curves for the temperature correlation for a set of jet fires with Q ranging from 3 to 6.4 MW. As can be seen, all cases follow the general equation (1) and a, b and c are the corresponding constants for each Q (Table 1). In all cases, the

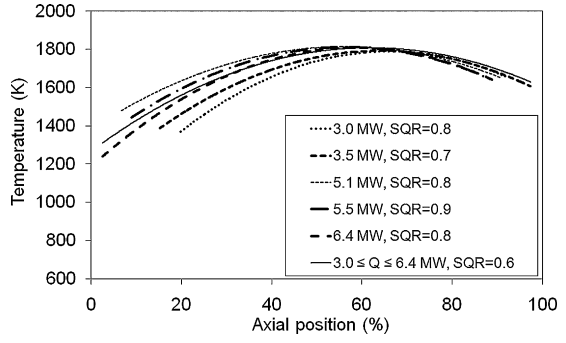

Fig. 5. Temperature variation (Eq. (1)) as a function of the axial position (d = 12.75 and 15 mm).

Table 1
Constants for Eq. (2).

Q (MW)	a	b	c
3.0	935	25.8	0.19
3.5	1100	21.6	0.17
5.1	1385	15.3	0.14
5.5	1290	18.5	0.16
6.4	1190	21.2	0.18
3.0–6.4	1270	17.4	0.14
8.5–9.6	980	29.1	0.27

maximum temperatures were recorded above the central part of the flame, at 60% < p < 70%, and reached values of approximately 1800 K. At the bottom of the flame the temperature increases continuously with height, because the oxygen/fuel mixture is improving as the axial distance from the exit orifice increases. At the central part of the flame, the oxygen/fuel mixture balance is the best one, and the highest temperatures are reached. Over the last part of the flame, the quality of the combustion starts to decrease because the mixture becomes poor in fuel and, as a result, the temperature decreases. The variation between the correlation lines can be due to the data scattering, but the trend remains clear; R^2 ranged between 0.7 and 0.9, which is a very good approximation to the experimental behaviour.

An acceptable general equation for this range of fuel mass flow rates can be obtained using the following values: a = 1269, b = 17 and c = 0.14, with a value of R^2 = 0.6.

4. Flame temperature as a function of the nominal heat release rate Q

The influence of the nominal heat release rate Q on the centreline temperatures was also analysed. In the lower region of the flames (0% < p < 40%) the temperature at a given point increased with Q and reached a maximum value, after which it decreased again as Q increased. The same behaviour – although with a smaller variation – was observed in the upper region (70% < p < 100%). However, in the region at which the maximum temperature was reached (60% < p < 70%) the variation between the different lines was very small or even null, i.e. the maximum temperature reached along the jet fire centreline was essentially the same at the diverse Q (Fig. 6), even though the different values of Q produced different flame sizes.

Fig. 6 shows the behaviour in the region in which the maximum temperatures were reached for some Q values (between 3 and 6.4 MW). The temperature over the range 60% < p < 70% of the centreline is essentially constant at all values of Q (i.e. for all flame lengths considered).

Fig. 7 shows a plot of a set of experimental values corresponding to different flame centreline locations and jet outlet orifice diameters. Although a considerable degree of scattering is observed, the

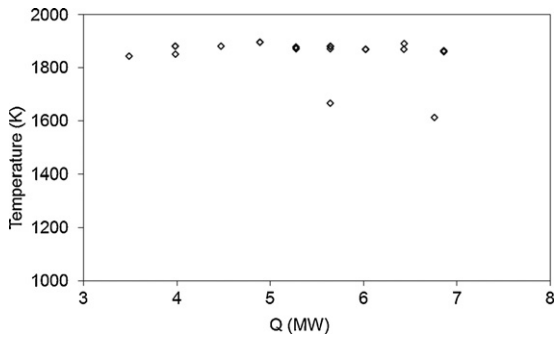

Fig. 6. T variation as a function of Q on Region II, for 3 ≤ Q ≤ 6.4 MW.

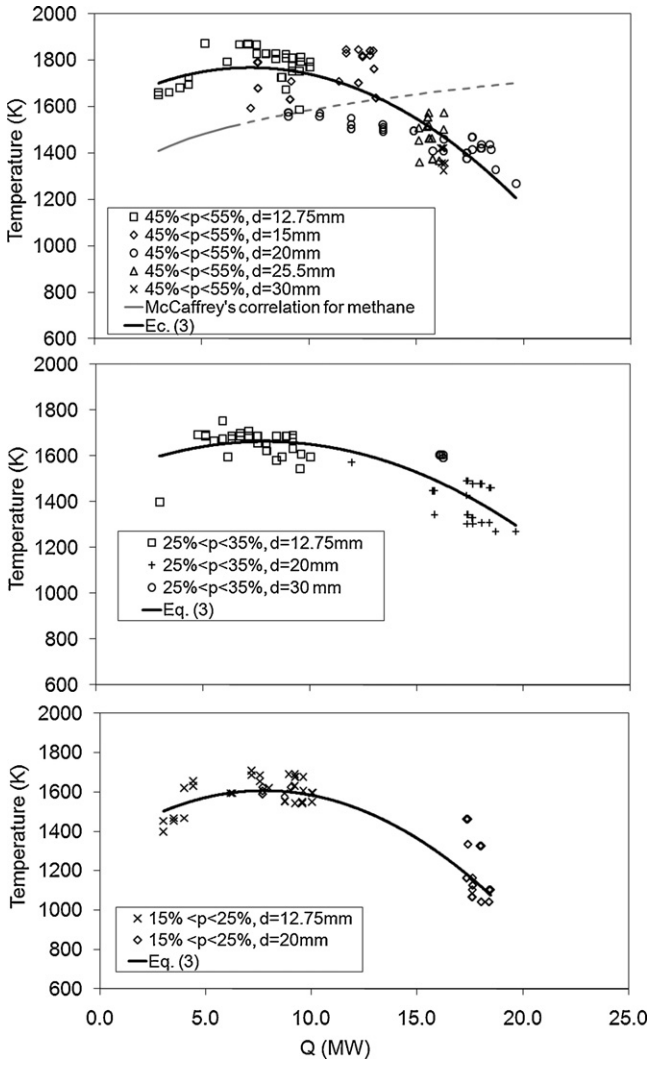

Fig. 7. Jet fire temperature as a function of the axial position and *Q*.

general trend of these data is quite consistent. It should be noted that the Froude number, a dimensionless group used sometimes when plotting jet fires experimental results, cannot be used here, as all data were obtained at sonic values. This figure shows clearly that the jet outlet diameter has no influence on the temperature behaviour.

As can be seen in Fig. 7, the temperature at a given location (p) increased with Q (i.e with the flame length), reached a maximum and decreased significantly at higher values of Q. The highest temperatures were recorded in the middle values of Q. The lowest temperatures were always measured at the highest Q values. This may be due to an excess of fuel in the fuel/air mixture, which led to poor combustion.

This trend is similar to that shown by the results published by McCaffrey [7] with natural gas, who found an increasing trend of T as a function of Q. However, the experimental results of this author were restricted to the lower range of values covered in this paper (this behaviour corresponds to the lowest values of Q in Fig. 7); this is why he did not realize that at higher values of Q the temperature decreases.

The behaviour shown in Fig. 7 is similar to that of the data obtained for natural gas by Gore et al. [12], who used larger exit diameters (76–102 mm). The temperature variations at different values of Q can also be described using a second-degree polynomial

Table 2
Constants for Eq. (3).

Axial position range (%)	*A*	*B*	*C*
15–25%	1330	71.4	4.6
25–35%	1500	41.9	2.7
45–55%	1575	53.2	3.7
40–60%	1650	36.3	3.0

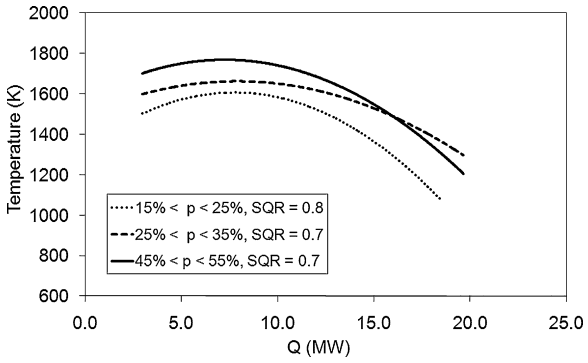

Fig. 8. Temperature variation correlations as a function of *Q*.

with the following general form:

$$T = A + BQ - CQ^2 \quad (3)$$

where T is the temperature in degrees Kelvin, and A, B and C are the corresponding coefficients for each axial position range. Table 2 shows the coefficients for some axial position ranges.

The prediction from Eq. (3) is plotted in Fig. 8 for each flame region. Despite the data scattering mentioned above, the predicted trend is acceptable for the range of Q analysed here, jet fire centreline positions and outlet diameters.

5. Conclusions

It is rather difficult to measure the flame temperature in a large jet fire due to the turbulence and movement of the flames. These characteristics produce a significant scattering of the experimental data, although the results obtained can be considered to be representative of large sonic propane jet fires, as they were quite reproducible (although they were derived from a set of experiments carried out during different days, the trends in the thermal behaviour of the fire were consistent and clear). The behaviour of jet fires involving other fuels should be similar to that observed with propane, as can be seen from the McCaffrey's work with natural gas jet fires; however, this should be further studied.

The results obtained for large vertical jet fires (flame lengths up to 8 m), corresponding to sonic jet releases of propane, show that the centreline temperature varies considerably. Three regions were identified: (a) over Region I (p < 40%), the temperature increased with the axial position; (b) over Region II (40% < p < 70%), the temperature varied smoothly and reached its maximum values, with an average value of approximately 1800 K and maximum values of 1900 K; and (c) over Region III (p > 70%), the temperature decreased, and the values measured at the tip of the flame were considerably higher than those measured at the bottom. Thus, the results offer a good picture of the axial temperature propane flame behaviour (momentum dominated).

This behaviour can be attributed to the following two factors: the improvement in fuel/air mixing along the jet fire, with a relatively low concentration of oxygen in Region I and a much better ratio in

Region II; and the low fuel concentration (due to fuel consumption) in Region III. The progressive increase in gas temperature along the jet also influenced the behaviour, since the gas entering Region I was cold, whereas most of the gas entering Regions II and III was hot.

When propane is used, the temperature variation as a function of the position on the flame centreline can be predicted accurately using a polynomial expression (Eq. (1)).

The jet fire length increased with Q. However, the maximum centreline temperatures reached (~1900 K, which corresponds approximately to the $60\% < p < 70\%$ region) were almost identical for all Q values. Nevertheless, in the lower and upper regions, the temperature at a given reduced length (p) increased with Q and reached a maximum value, after which it decreased again as Q increased. Eq. (3) is proposed to predict this behaviour. The jet outlet diameter had no influence on the temperature behaviour.

Acknowledgments

The authors are grateful to the Spanish Ministry of Education and Science for funding provided under project CTQ2005-06231, and for the doctoral grant awarded to M. G.-M).

References

[1] R.M. Darbra, J. Casal, Saf. Sci. 42 (2004) 85–98.
[2] G.A. Chamberlain, Controlling Hydrocarbon Fires in Offshore Structures, 2002, OTC 14132.
[3] L.T. Cowley, M.J. Pritchard, Large scale natural gas and LPG jet fires and thermal impact on structures, Gastech 90, in: 14th International LNG/LPG Conference, Amsterdam, 1990.
[4] N. Davenport, Large scale natural gas/butane mixed fuel jet fires, Final Report to the European Commission, 1994, Shell Research Report no. TNER.94.030.
[5] M. Gómez-Mares, L. Zárate, J. Casal, Fire Saf. J. 43 (2008) 583–588.
[6] O.K. Sonju, J. Hustad, Norwegian Marit. Res. 4 (1984) 2–11.
[7] B.J. McCaffrey, Combust. Sci. Technol. 63 (1989) 315–335.
[8] A. Santos, M. Costa, Combust. Flame 142 (2005) 160–169.
[9] D.B. Pfenning, Final Report for Blowout Fire Simulation Tests, NBS-GCR-85-484, National Bureau of Standards, Gaithersburg, Maryland, 1985, 200899.
[10] T.A. Brzustowski, S.R. Gollahalli, M.E. Kaptein, H.F. Sullivan, M.P. Gupta, Radiant Heating from Flares, ASME Heat Transfer Conference, 1975, 75-HT-4.
[11] H.A. Becker, S. Yamazaki, Combust. Flame 33 (1978) 123–149.
[12] J.P. Gore, G.M. Faeth, D. Evans, D.B. Pfenning, Structure and radiation properties of large-scale natural gas/air diffusion flames, Fire Mater. 10 (1986) 161–169.
[13] L.G. Blevins, W.M. Pitts, Fire Saf. J. 33 (1999) 239–259.
[14] S. Brohez, C. Delvosalle, G. Marlair, Fire Saf. J. 39 (2004) 399–411.
[15] M.A. Muñoz, Estudio de los parámetros que intervienen en la modelización de los efectos de grandes incendios de hidrocarburo: geometría y radiación térmica de la llama. Ph.D. thesis. Universitat Politècnica de Catalunya. Barcelona, 2005.
[16] A. Palacios, M. Muñoz, J. Casal, AIChe J. 55 (1) (2009) 256–263.
[17] W. Meier, R.S. Barlow, Y.L. Chen, J.Y. Chen, Combust. Flame 123 (2000) 326–343.
[18] D. Drysdale, An Introduction to Fire Dynamics, John Wiley and Sons, England, 1994, ISBN 0471906131.